Measurement Science and Technology

PAPER • **OPEN ACCESS**

Projected moving patterns for reference-free background-oriented schlieren technique (BOS)

To cite this article: Markus Raffel *et al* 2024 *Meas. Sci. Technol.* **35** 115306

OPEN ACCESS
IOP Publishing
Measurement Science and Technology
Meas. Sci. Technol. **35** (2024) 115306 (9pp)
https://doi.org/10.1088/1361-6501/ad7165

Projected moving patterns for reference-free background-oriented schlieren technique (BOS)

Markus Raffel[1,*], Nathanial T Smith[2], C Christian Wolf[1], James T Heineck[2] and Anthony D Gardner[1]

[1] Institute of Aerodynamics and Flow Technology, DLR, Göttingen, Germany
[2] Experimental Aero-Physics Branch, NASA Ames Research Center, Moffett Field, CA, United States of America

E-mail: Markus.raffel@dlr.de

Received 25 May 2024, revised 13 August 2024
Accepted for publication 20 August 2024
Published 29 August 2024

Abstract

A background-oriented schlieren technique (BOS) using projected background patterns is presented. The projected backgrounds can be scaled to the measurement requirements, providing greater flexibility than printed backgrounds. The evaluation of the BOS image pairs using cross-correlation or optical flow analysis was demonstrated to produce equivalent results. The background pattern can dynamically be shifted by a rotating mirror, allowing evaluation using the reference-free shadowgraphy or reference-free BOS methods. The forward BOS technique is demonstrated, in which a projected speckle pattern is illuminated through a density object and recorded by a camera focused on the screen. In contrast to standard shadowgraphy, where the local image intensity is the parameter proportional the second derivative of density, this technique is robust with respect to varying lighting of the field as long as the displacement of small-scale image structures can be determined.

Keywords: BOS recording, BOS processing, schlieren technique, laser speckles, density gradients

1. Introduction

The principle of the background-oriented schlieren (BOS) technique is based on the variation of the refractive index of air as a result of density gradients. In a first step, a reference image is generated by capturing a suitable background in still air [1]. In a subsequent additional image, the same background is then imaged through an object with a density gradient. These two images can then be analysed using windowing cross-correlation (CC) methods. The advantage of such a method is that extremely robust correlation algorithms [2, 3], which were developed to analyse particle image velocimetry measurements, are reused to determine the deflection of the light rays without significant additional effort.

Assuming paraxial imaging and a sufficiently small deflection of the light rays, equation (1) can be derived for the offset of the image positions. The deflection of the rays produces an offset of the image spots between the reference and the measurement image, Δy, which can be interpreted as the density gradient of the flow as integrated along the optical path during the image acquisition

$$\Delta y = f\left(\frac{z_D}{z_D + z_A - f}\right)\varepsilon \tag{1}$$

where the light beam deflection angle is:

$$\varepsilon = \frac{1}{n_0}\int_0^1 \frac{\partial n}{\partial y}\mathrm{d}z. \tag{2}$$

* Author to whom any correspondence should be addressed.

The equations use the focal length, f, the distance between background and density gradient, z_D, and the distance between density gradient and lens, z_A, according to the optical setup.

The BOS technique however, has several drawbacks with respect to classical schlieren techniques [4].

1. The evaluation window size limits the spatial measurement resolution and therefore imposes a spatial filter on the data.
2. The common BOS techniques require a reference image taken with undisturbed flow.
3. An additional spatial filtering of the data occurs due to the requirement to focus on the background and not on the imaged object.
4. Additionally, to the comments by [4], the requirement to size and print a separate background for each experiment or find a suitable natural background [5] can be onerous.

A close relative of BOS is 'density speckle photography' (DSP), as described by Debrus *et al* and Köpf [6, 7] and in an improved version by Wernekinck and Merzkirch [8]. The laser-based DSP measurement method uses projected, expanded laser beams to illuminate the flow field and analyses the offset of the laser speckles on a ground glass screen to visualise the variation of the refractive index.

The authors of this paper propose the use of projected backgrounds analogue to those used for DSP. In comparison to printed backgrounds, the projected backgrounds can be moved at high speed if desired, for example using a rotating mirror, and dynamically adjusted in terms of field size (slide projection) or in terms of field size and pattern coarseness (speckle projection). An image analysis via optical flow (OF) techniques [9, 10] is compared to standard CC algorithms. OF techniques do not depend on a minimum correlation window size and, hence, provides a better spatial resolution at the cost of a reduced robustness. The moving background pattern enables applying the reference-free digital BOS method, which evaluates measurement images with a short time delay and eliminates the need for a reference image [11].

2. Projected moving background pattern BOS

The BOS method proposed employs a projection of a random dot pattern from a photographic slide onto the background similar to the background illustrated in figure 1. Additionally, the background pattern is translated using a rotating mirror in the projection system. As illustrated in figure 2, if the position of an individual fraction of the projected background pattern moves between two image recordings due to the rotating mirror, it will be seen through a different part of the density object. This can be evaluated as reference-free digital shadowgraphy using a moving BOS background, as presented by Gardner *et al* [12], or as BOS or knife-edge images by various techniques, as described in the following sections. If a series of images is taken over a time frame in which the flow can be considered steady, either by using fast acquisition or a steady flow, then the ensemble correlation of Meinhart *et al* [13] can be used to reduce the window size to the range 4×4–8×8 pixels. A comparable subtraction method has been used by Settles and Hargather [4], although the moving background method utilized here represents a novel approach. Multiple images have been employed in schlieren velocimetry by Mittelstaedt *et al* [14], yet the ensemble correlation was not employed in that instance. The AIRBOS method of Smith *et al* [10] employed OF algorithms to achieve comparable outcomes, yet it did not utilize projection to generate the motion of background patterns.

The apparatus for the moving projected background pattern test on a burning candle consisted of a rotating mirror system, a Phantom VEO 640 camera recording at a framerate of 3 kHz at an image size of 1024×1600 pixels. The exposure time was set to 150 µs. The lens utilized was a Nikkor with a focal length of 50 mm and an aperture leading to a f-number of 8. The distance between the camera and the candle was 0.80 m, while the distance between the camera and the background was 1.60 m. The background pattern was generated by a slide projector and a slide of a random dot background pattern. The rotating mirror was operated at 0.33 revs s^{-1} . The background pattern exhibited a displacement of approximately 8.5 pixels in the image plane between two subsequent recordings. A series of 201 images was recorded for the evaluation, resulting in a total of 200 results containing the background displacement between subsequent images.

OF is the apparent motion between images due to changes in brightness. To determine the displacement between image pairs, we employ a regularization-based Horn–Schunck [15] type algorithm. A penalty function of the velocity gradients is weighted against a brightness constancy term which is used to enforce smoothness. Due to the large background displacement between images, a coarse-to-fine pyramidal scheme is required. Image pyramids are constructed for each image pair. Methods such as a pyramidal scheme are required for OF applications where motions exceed approximately 1–2 pixel per frame, BOS or otherwise to accurately solve the displacements. The solution is calculated on the coarsest level, and the OF at each level is used to warp the second image towards the first image on the next finest scale. A penalty weight of 200 and five pyramid levels are used to compute the flow between image pairs. It has been found that this value, while it may result in increased noise in the individual solutions, can prevent the blurring of finer scale structures. Increasing the penalty weight can have a similar effect to that of increasing the window size in CC methods. However, our experience has shown that weighting is much more subjective and can differ between BOS data sets. This subjectivity of penalty weighting is common to regularization-based methods. It has been observed in the current and previous work that the use of multiple backgrounds or solution averaging can result in the cancellation of noise, while simultaneously revealing smaller-scale schlieren in cases where they are present.

The results of the more conventional displacement evaluation performed at DLR are based on a sequential CC performed with the LaVision DaVis 10 software [16], using a multi-pass correlation down to 12×12 pixels with 75% overlap. This approach yields a grid spacing of 3 pixels in both the x- and y-directions, in comparison to the single-pixel resolution of the OF method.

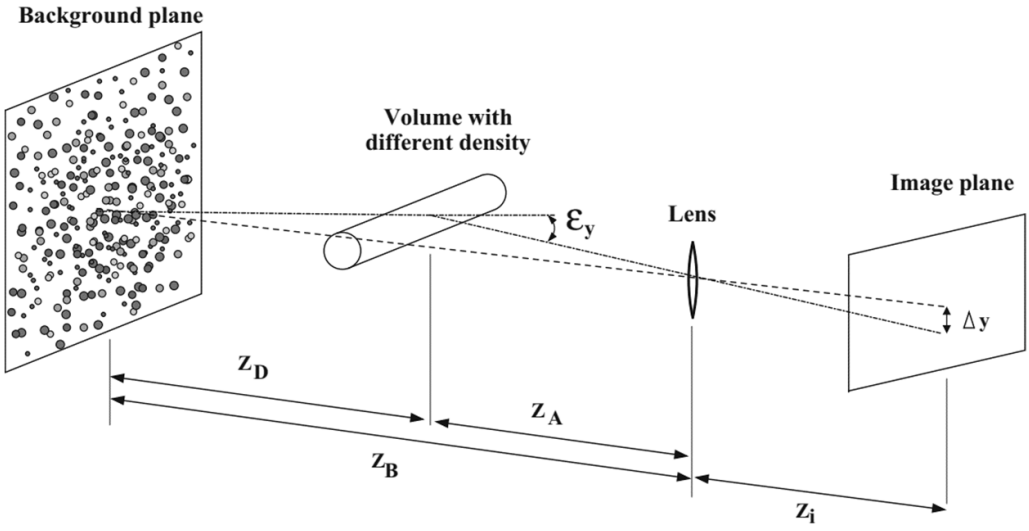

Figure 1. Recording principle of the conventional background-oriented schlieren method BOS [1].

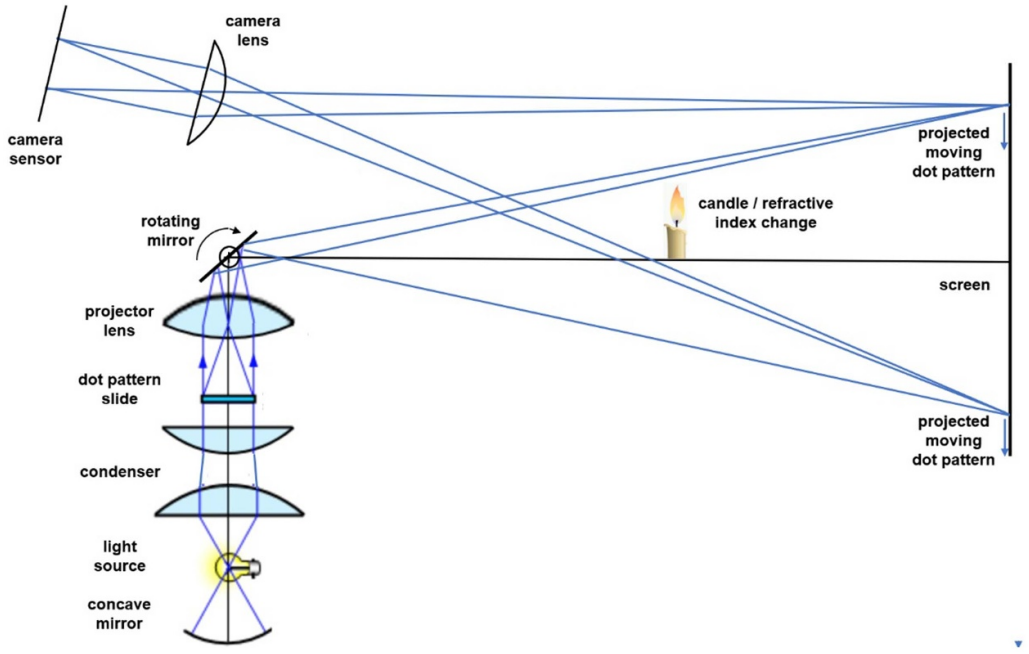

Figure 2. Reference-free BOS using a slide projector and a rotating mirror for a moving background pattern.

Figure 3 shows sample results for the horizontal motion, Δx, and five different evaluation strategies(a) to (e) using CC (CC, top row) or OF (OF, bottom row). In each result, the candle flame and its plume are in the centre. The average right-to-left background motion of about -8.5 pixels was subtracted. The result is in the range between -1.5 and 1.5 pixels, representing the second derivative of the density, $\Delta^2\rho/\Delta x^2$, as argued by Gardner *et al* [12]. It is noted that all results in figure 3 contain a shadow-like, mirror-inverted image of the density gradients in the right half. This effect will be explained and utilized as 'forward BOS' in the next chapter, in which the slide projector is replaced with a pointwise laser light source. It is also noted that in general, the evaluation noise in the left side of each image is larger than in the right side due to the illumination being not perfectly homogeneous and slightly darker on the left.

Results (a) and (d) correspond to 'simple' instantaneous results derived from two successive camera images N and $N + 1$. Background noise is visible in both results, with slightly less noise in case of the OF evaluation, despite its finer grid resolution (1 pixel versus 3 pixels).

The candle plume is laminar at the bottom and turbulent at the top, but the unsteadiness is slow compared to the image acquisition rate. Hence, the noise can be suppressed at the cost of temporal resolution by combining more than two images via sliding-window methods. Figure 3(b)) uses a sum-of-correlation ('ensemble correlation', Santiago *et al* [17]) approach, averaging the correlation planes in images

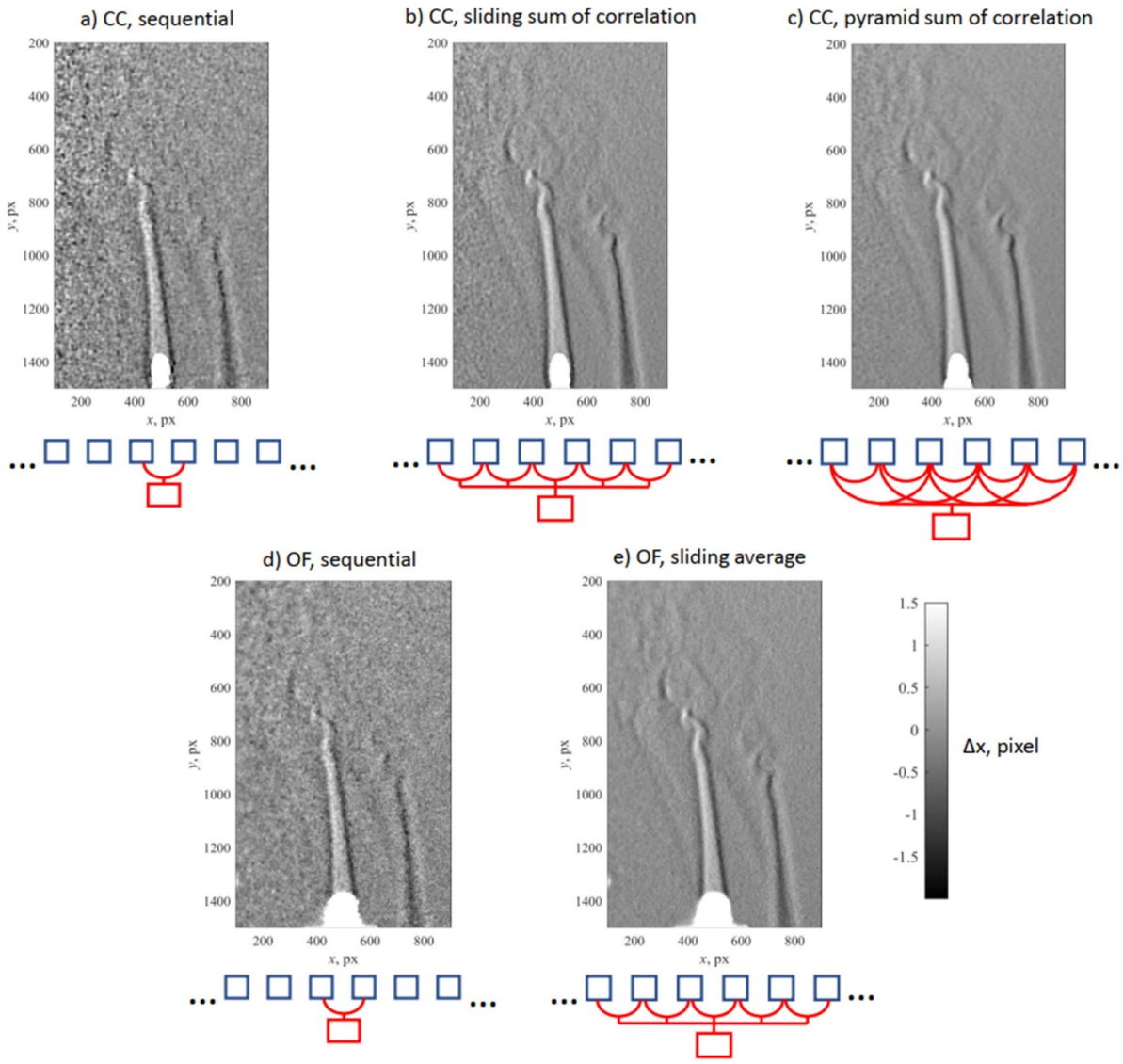

Figure 3. Instantaneous results of the candle test case, different evaluation strategies using cross-correlation (CC), top row, and optical flow (OF), bottom row.

$N \pm 2$ before peak detection. The noise suppression is obvious, while maintaining or even pronouncing instantaneous turbulent structures. Averaging instantaneous OF results in a sliding window of the same size yields a comparable result, seen in figure 3(e)).

Figure 3(c) repeats the sum-of-correlation approach, additionally accounting for correlations between images N and $N + 2$. This approach can be termed 'pyramid level 2' after Sciacchitano *et al* [18]. Correlation noise is further suppressed by adding additional correlation planes, but the inherent averaging over longer time spans starts to reduce the intensity of the small-scale turbulent structure's signal.

The plot in figure 4 shows the horizontal background motion versus the horizontal coordinate, extracted and averaged over the vertical y-range in the red rectangle situated in the laminar region of the flame plume. The labels a) to e) repeat the different evaluation strategies from figure 3. The quantitative agreement of all methods is good and supports the previous observations: the noise level in the instantaneous results, (a) and (d), can be suppressed by the sliding window techniques,(b) and (e), but further temporal averaging leads to smaller peak levels, (c).

3. Laser speckle pattern BOS

A schematic of the forward BOS setup is shown in figure 5, where the phase object was a horizontal helium jet emitted from a small plastic tube. The distance from the camera to the jet was about 0.8 m, and the distance between the jet and the background was about 0.4 m. The camera's field of view included both the image of the tube itself in the lower part (in 'standard' BOS schlieren images, the jet refracts rays from the background to the camera) and the shadow of the tube in the upper part. The latter effect, where the jet refracts rays from the light source to the background, will be referred to as 'forward' BOS schlieren images in the remainder of this article.

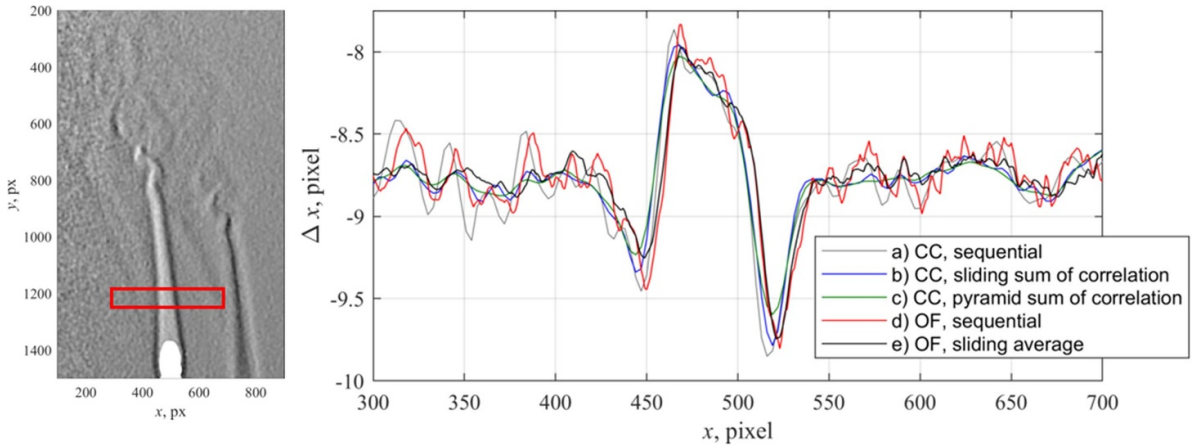

Figure 4. Horizontal background motion Δx along x, extracted and averaged from figure 3, $y = 1200$–1250 px.

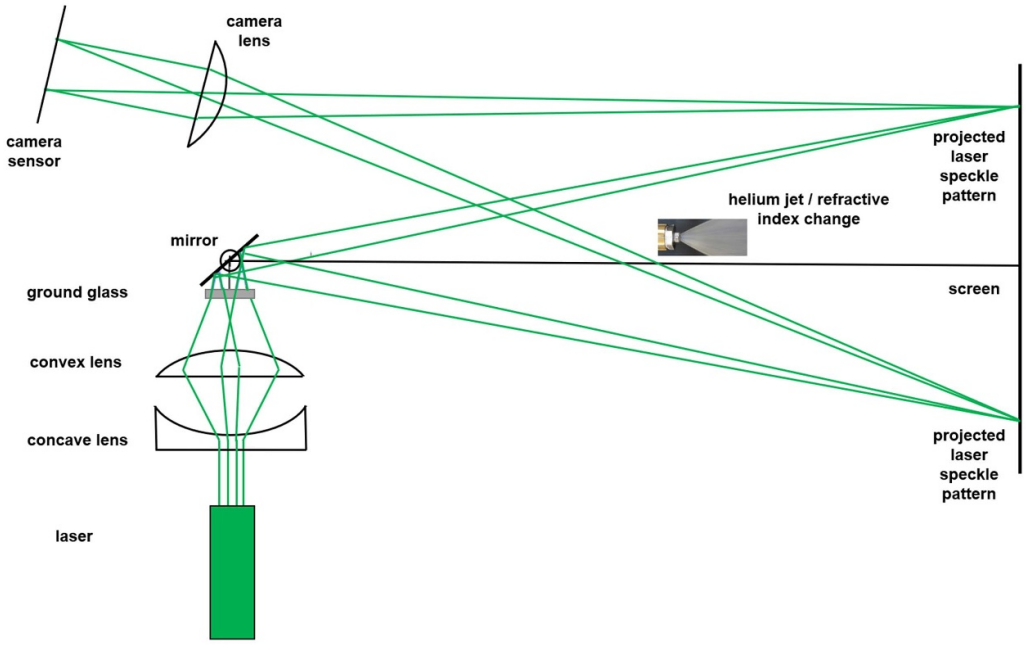

Figure 5. Reference-free BOS using a laser and a rotating mirror for a moving speckle background pattern.

The forward BOS images are similar to shadowgraphs, but the laser light transmitted through the phase object contains an intensity pattern created by a ground glass placed in front of the laser. By adjusting the lenses between the laser and the screen, the density and size of the projected speckles can be controlled [19]. The smaller the laser spot on the screen, the larger the speckle size and vice versa. Smaller laser spots also result in a greater depth of field of the projection, allowing the location of the density field to be varied widely without noticeably blurring either the shadow of the nozzle or the data. The laser used was a Spectra Physics Excelsior with 250 mW at 532 nm and a beam diameter of 0.32 mm. Focal lenses of -25 mm and 100 mm and a beam expander were used. The total size of the illuminated field can be increased by using lenses with shorter focal lengths.

Figure 6 compares the relevant parts of the light path for the standard (top) and forward BOS methods (bottom). Note that the apparent motion of the background pattern as observed by a camera has opposite signs, e.g. a low-density phase object contracts background structures in standard mode, but expands background structures in forward mode. This explains the mirror-inverted, shadow-like candle plume seen in figure 4.

The camera used was a Phantom VEO640 (same as in the first candle experiment) at 2 kHz, the lens was a Zeiss Milvus $f = 100$ mm, and the focus was on the background. A rotating mirror was placed in the light path of the laser to allow background motion as demonstrated in the previous section, but during the recordings discussed in this section the mirror was fixed. Therefore, the evaluation shows the displacements between the reference image (helium jet turned off) and the measurement images (helium jet turned on), and the result represents the first derivative of the density (here: $\Delta\rho/\Delta y$) instead of the second derivative ($\Delta^2\rho/\Delta y^2$).

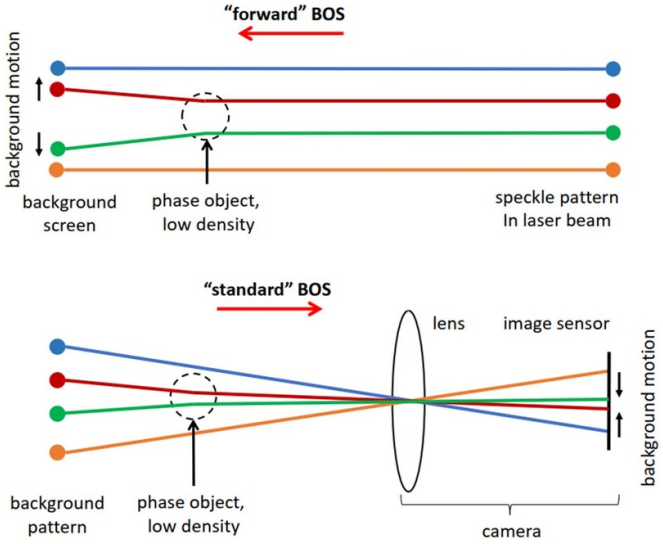

Figure 6. Comparison of the principles for forward BOS (top) and standard BOS (bottom).

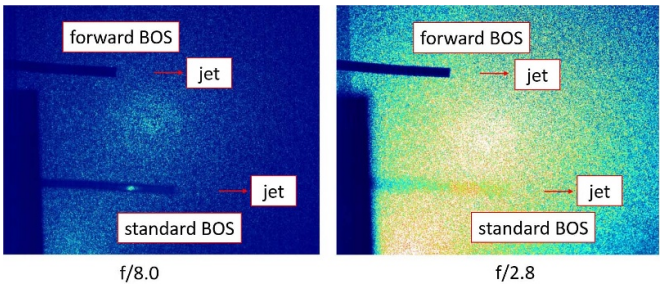

Figure 7. Sample camera images of the helium jet and laser speckle background for camera lens apertures $f/8.0$ (left) and $f/2.8$ (right). The jet tube and its shadow are visible in separate areas of the image, enabling standard and forward BOS in the same image.

Figure 7 shows two example images for two different aperture settings of the camera lens, *f*/8.0 (left) and *f*/2.8 (right). In both cases, the laser speckle pattern was generated by a ground glass diffuser and projected onto the background using the non-rotating mirror. The camera was focused on the background and is not collinear with the laser beam, but placed above it, so that the image of the jet tube (standard BOS) and its shadow (forward BOS) appear on top of each other. Note that the helium tube is almost invisible at $f/2.8$ due to the small depth of field. As expected, the image is much brighter at $f/2.8$ than at $f/8.0$, since the aperture opening increases by a factor of more than 8. This is partly compensated by reducing the exposure time from 1500 µs to 500 µs, and, thus, reducing possible motion blur. Both images are displayed with the same colour coding in a range of 0–1000 counts.

Figure 8 depicts three different evaluation results based on a comparison between an instantaneous measurement image and the jet-free reference image for a stationary laser speckle background pattern and an aperture setting of $f/8.0$. The grayscale corresponds to the vertical background shift Δy in the range of -1.5 to 1.5 pixels. The displacement magnitudes of standard BOS (bottom) and forward BOS (top) are similar, since both depend on the distance between the phase object and the background, but the direction is mirror-inverted as predicted in figure 6. Note that the geometric scaling of the forward and standard BOS images was not calibrated.

The CC in figure 8(a)) used the same parameters as in the candle test case, which means that the grid resolution is three times lower in both x- and y-directions compared to the OF result of figure 8(b)). Nevertheless, both evaluations visualize to some extent the instantaneous turbulent structures within the jet. A closer look reveals that the forward BOS result is sharper than the standard BOS result because the camera is focused on the background. The result in figure 8(c) uses the OF algorithm without the pyramidal evaluation scheme described in section 2.

The results shown in figure 9 represent non-ensemble averages calculated from 500 individual results. The average y-displacement along the y-coordinate is shown in figure 10 for two selected areas (red boxes) in the standard and forward BOS regions. The similar magnitudes but opposite signs for both methods are confirmed, as well as the very good quantitative agreement between the CC (red lines) and the OF with the pyramidal scheme (black lines). Omitting the pyramidal scheme (blue lines) leads to an underestimation of the background shift.

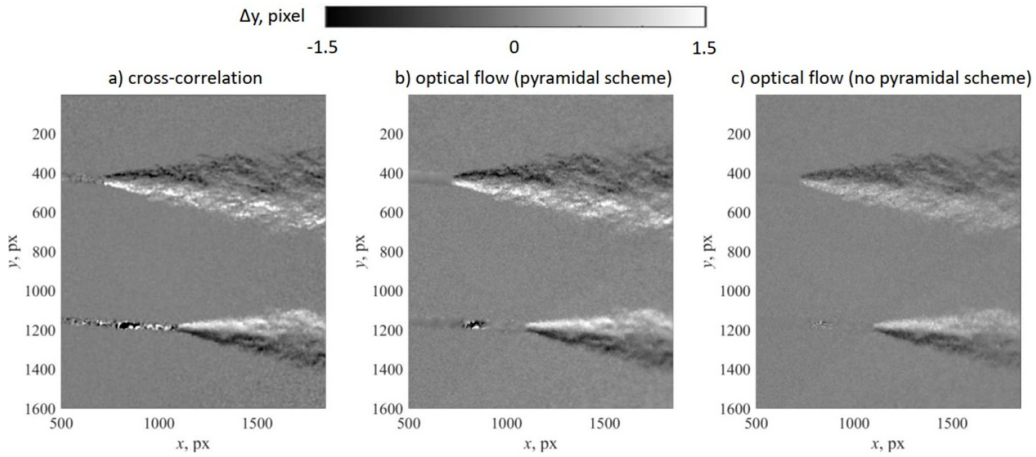

Figure 8. Instantaneous sample result of the helium jet, $f/8.0$.

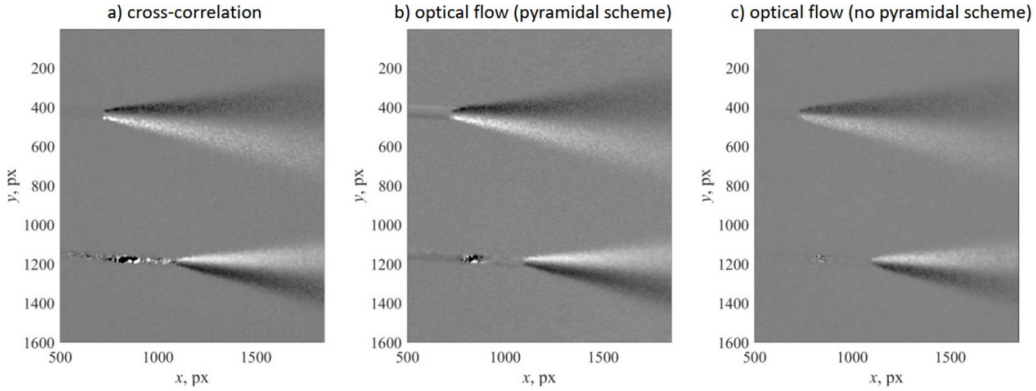

Figure 9. Averaged result of the helium jet, 500 individual samples, $f/8.0$.

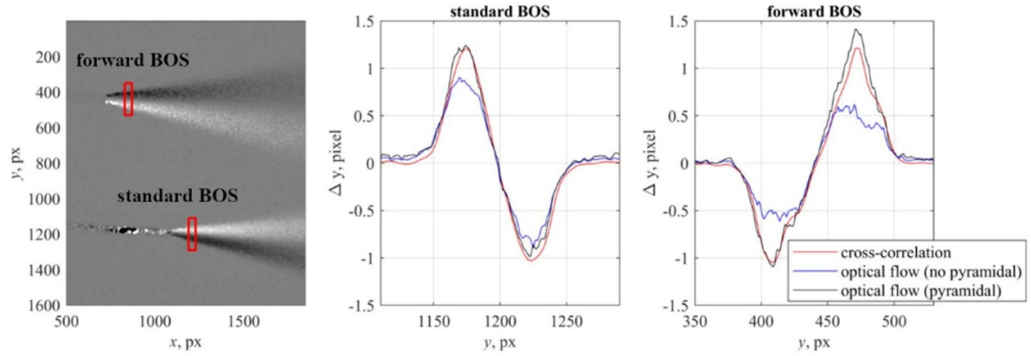

Figure 10. Vertical profiles (centre, right) of the averaged result (left, repeated from figure 9(a)), different evaluation schemes.

When opening the aperture from $f/8.0$ to $f/2.8$, as seen in figure 11, it can be observed that the standard BOS images of the density gradients in the lower half appear blurred and have less signal due to a smaller depth of focus, with the focus set on the background. In contrast, the forward BOS mode, represented by the gradients in the upper half of the images, produces more image displacement (more signal) and therefore appears slightly crisper. The reasons for this are not yet clear, but are probably related to the shorter exposure times (better representation of instantaneous turbulent structures) and the brighter background (better signal-to-noise ratio). The line plots in figure 12 compare $f/8.0$ (dashed lines) and $f/2.8$ (solid lines), confirming that opening the aperture greatly reduces the standard BOS signal, but slightly increases the forward BOS signal. The fact that only increases in the negative displacement direction is considered to be a consequence of the helium jet varying slightly over time. A Again, the good quantitative agreement between the CC and the pyramidal scheme OF is highlighted.

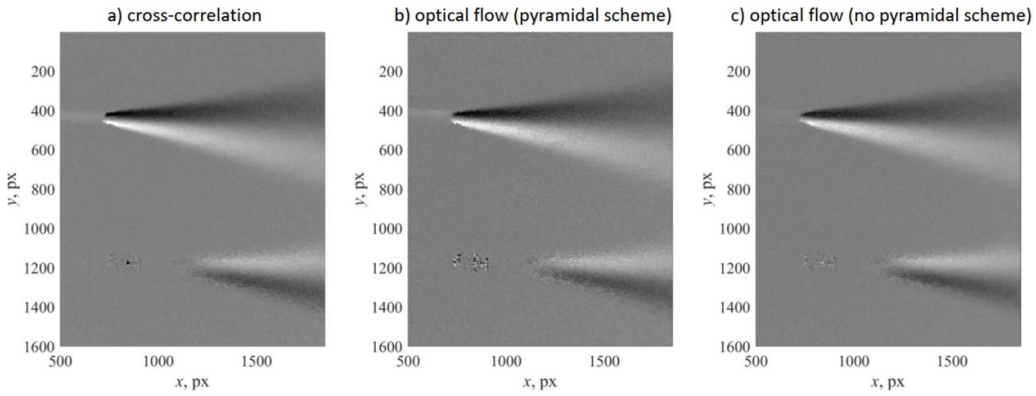

Figure 11. Averaged result of the helium jet, 500 individual samples, $f/2.8$.

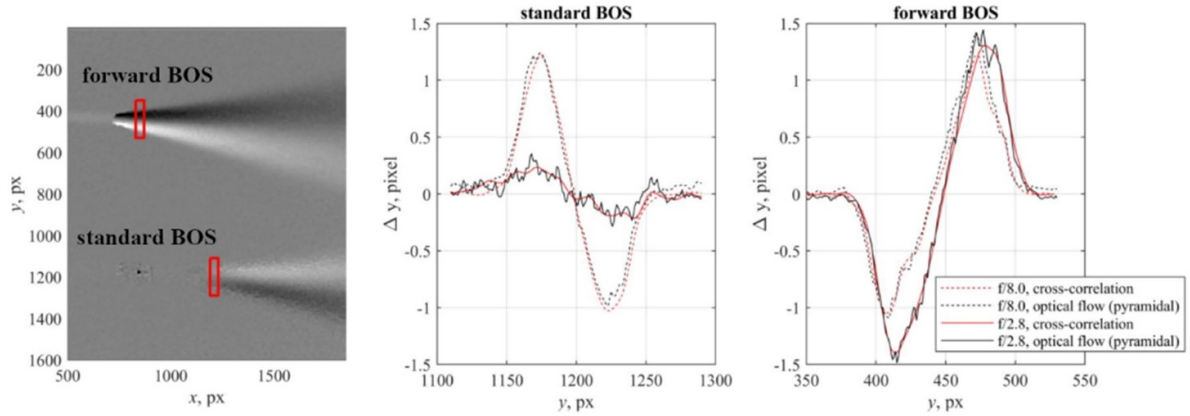

Figure 12. Vertical profiles (centre, right) of the averaged result (left, repeated from figure 11(a)) for $f/8.0$ and $f/2.8$.

4. Conclusion

This article demonstrates the benefits of projected backgrounds for BOS. The main results and advantages are:

1. The projected backgrounds provide a greater flexibility compared to static printed backgrounds, which are often permanently installed, e.g. affixed to a wind tunnel side wall. Preparing photographic slides with different patterns or using a digital projector (the latter approach was not used in the current work) enables easier ad-hoc adjustments during a measurement campaign. This particularly holds true for large-scale backgrounds or restricted access to the test environment.
2. Laser speckle backgrounds provide additional options in terms of illumination intensity or adjustable background coarseness.
3. The background can be moved dynamically, e.g. by a rotating mirror, allowing evaluation with reference-free shadowgraph or reference-free BOS methods.
4. Forward BOS using projected backgrounds is shown in this paper. The projected speckle pattern shines through the density object and is captured by a camera focused on the screen. Unlike standard shadowgraphy, this technique is robust when the illumination of the field is uneven, and the point motion is related to the first derivative of the density.
5. Evaluation of backgrounds with a density object is shown using CC or OF analysis of image pairs, showing equivalent results. Ensemble or simple averaging is shown to improve the signal for static flows.

Data availability statement

The data cannot be made publicly available upon publication due to legal restrictions preventing unrestricted public distribution. The data that support the findings of this study are available upon reasonable request from the authors.

Acknowledgments

The authors would like to acknowledge the continued support of the decades-long U.S.-German collaboration by NASA and DLR leadership.

Conflict of interest

The authors declare no conflict of interest.

ORCID iDs

Markus Raffel https://orcid.org/0000-0002-3340-9115
C Christian Wolf https://orcid.org/0000-0002-9052-7548
Anthony D Gardner https://orcid.org/0000-0002-1176-3447

References

[1] Raffel M 2015 Background-oriented schlieren (BOS) techniques *Exp. Fluids* **56** 60
[2] Settles G S 2018 Smartphone schlieren and shadowgraph imaging *Opt. Lasers Eng.* **104** 9–21
[3] Bauknecht A, Merz C B and Raffel M 2016 Airborne visualization of helicopter blade tip vortices *J. Vis.* **20** 139–50
[4] Settles G S and Hargather M J 2017 A review of recent developments in schlieren and shadowgraph techniques *Meas. Sci. Technol.* **28** 042001
[5] Bauknecht A, Merz C, Raffel M, Landolt A and Meier A H 2014 Blade-tip vortex detection in maneuvering flight using the background-oriented Schlieren technique *J. Aircr.* **51** 2005–14
[6] Debrus S, Françon M, Grover C P, May M and Roblin M L 1972 Ground glass differential interferometer *Appl. Opt.* **11** 853–7
[7] Köpf U 1972 Application of speckling for measuring the deflection of laser light by phase objects *Opt. Commun.* **5** 347–50
[8] Wernekinck U and Merzkirch W 1987 Speckle photography of spatially extended refractive-index fields *Appl. Opt.* **26** 31–32
[9] Hill M A and Haering E A 2017 Ground-to-air flow visualization using solar calcium-K line background-oriented schlieren *Exp. Fluids* **58** 4
[10] Smith N T, Heineck J T and Schairer E T 2017 Optical flow for flight and wind tunnel background oriented schlieren imaging *55th AIAA Aerospace Sciences Meeting* (*Grapevine, TX*) (https://doi.org/10.2514/6.2017-0472)
[11] Raffel M Tung C Richard H, Yu Y and Meier G E A 2000 Background oriented stereoscopic schlieren (BOSS) for full-scale helicopter vortex characterization *9th Int. Symp. on Flow Visualization* (*Edinburgh, UK*)
[12] Gardner A D, Raffel M, Schwarz C, Braukmann J N and Wolf C C 2020 Reference-free digital shadowgraphy using a moving BOS background *Exp. Fluids* **61** 44
[13] Meinhart C D, Wereley S T and Santiago J G 2000 A PIV algorithm for estimating time-averaged velocity fields *J. Fluids Eng.* **122** 285–9
[14] Mittelstaedt E, Davaille A, van Keken P E, Gracias N and Escartin J 2010 A noninvasive method for measuring the velocity of diffuse hydrothermal flow by tracking moving refractive index anomalies *Geochem. Geophys. Geosystems.* **11** 10
[15] Horn B K P and Schunck B G 1981 Determining optical flow *Artif. Intell.* **17** 185–203
[16] LaVision GmbH 2019 Product manual for DaVis 10.1: flowmaster D10.1 (LaVision GmbH)
[17] Santiago J G, Wereley S T, Meinhart C D, Beebe D J and Adrian R J 1998 A particle image velocimetry system for microfluidics *Exp. Fluids* **25** 316–9
[18] Sciacchitano A, Scarano F and Wieneke B 2012 Multi-frame pyramid correlation for time-resolved PIV *Exp. Fluids* **53** 1087–105
[19] Meier A H and Roesgen T 2013 Improved background oriented schlieren imaging using speckle illumination *Exp. Fluids* **54** 1549